Physica A 512 (2018) 552–565

Contents lists available at ScienceDirect

Physica A

journal homepage: www.elsevier.com/locate/physa

A crucial role of long-range hydrodynamic interactions near the colloidal glass transition based on time-convolutionless mode-coupling theory

Michio Tokuyama [a,*], Takayuki Narumi [b], Junichi Kawamura [a]

[a] *Institute of Multidisciplinary Research for Advanced Materials, Tohoku University, Sendai 980-8577, Japan*
[b] *Graduate School of Sciences and Technology for Innovation, Yamaguchi University, Ube 755-8611, Japan*

HIGHLIGHTS

- Time-convolutionless mode-coupling theory is applied for colloidal suspensions.
- Nonlinear memory function consists of mechanical interactions and hydrodynamic interactions.
- Importance of long-range hydrodynamic interactions is emphasized.
- Theoretical prediction for a critical point is qualitatively consistent with that obtained from experimental data.

ARTICLE INFO

Article history:
Received 6 October 2016
Received in revised form 21 May 2018
Available online 11 August 2018

Keywords:
Colloidal suspensions
Hard spheres
Hydrodynamic interactions
Polydispersity
Time-convolutionless mode-coupling theory

ABSTRACT

The time-convolutionless mode-coupling theory (TMCT) recently proposed for molecular systems is employed to derive a TMCT equation for the collective-intermediate scattering function in suspensions of hard-sphere colloids from the nonlinear Langevin equations with the hydrodynamic interactions between colloids. The nonlinear memory function contained in the TMCT equation consists of two types of interactions between colloids; a mechanical interaction and a hydrodynamic interaction. It is predicted from the TMCT equation how the hydrodynamic interactions can affect the ergodic to non-ergodic transition at a critical point. Then, such a hydrodynamic effect is tested by the experimental data for suspensions of hard-sphere colloids with size polydispersities. Thus, it is emphasized that the long-range hydrodynamic interactions are indispensable to explain the polydispersity dependence of the experimental critical points which is quite different from that of simulations where only the mechanical interactions are taken into.

1. Introduction

A large number of fundamental works on suspensions of colloids have been performed experimentally [1–18] and theoretically [19–43]. Understanding their dynamics is one of important problems in soft matter science not only from an academic point of view as in fundamental colloidal physics but also from a practical point of view as in chemical engineering and biology. In most cases, however, the important effect of hydrodynamic interactions between colloids on their dynamics near the glass transition is not fully recognized yet.

In this paper, we apply the time-convolutionless mode-coupling theory (TMCT) [44–47] for suspension of hard-sphere colloids and derive the TMCT equation for the collective-intermediate scattering function, where the nonlinear memory

---

[*] Corresponding author.
E-mail address: tokuyama@tagen.tohoku.ac.jp (M. Tokuyama).

https://doi.org/10.1016/j.physa.2018.08.136
0378-4371/

function contains two different terms resulted from mechanical interactions and hydrodynamic interactions. We then show how the critical point (or kinetic glass transition point) is determined by two different interactions. In order to check the important role of the hydrodynamic interactions, we discuss the critical volume fraction $\phi_c(\sigma)$ for the suspension of polydisperse colloids, where σ is a size polydispersity. Then, the present theory predicts the following three cases for ϕ_c:

$$\begin{cases} \text{(i)} \quad \phi_c(\sigma) = \phi_h(\sigma) < \phi_c^{(m)}(\sigma), & \text{for } 0 \le \sigma < \sigma_0, \\ \text{(ii)} \quad \phi_c(\sigma) = \phi_h(\sigma) = \phi_c^{(m)}(\sigma), & \text{for } \sigma = \sigma_0, \\ \text{(iii)} \; \phi_c(\sigma) = \phi_h(\sigma) > \phi_c^{(m)}(\sigma), & \text{for } \sigma > \sigma_0. \end{cases} \tag{1}$$

where σ_0 is a constant to be determined. Here $\phi_c^{(m)}(\sigma)$ is a critical volume fraction obtained only from the mechanical interactions and is found from all the simulations, while $\phi_h(\sigma)$ is a critical volume fraction obtained from the correlation effect due to the long-range hydrodynamic interactions among colloids and is given by

$$\phi_h(\sigma) = \phi_h(0)(1 + 3\sigma^2) \tag{2}$$

with the hydrodynamic critical point at $\sigma = 0$ [20,21]

$$\phi_h(0) = (4/3)^3/(7\ln 3 - 8\ln 2 + 2) \simeq 0.571847\cdots, \tag{3}$$

where in order to obtain Eq. (2), the Gaussian distribution was assumed for particle radius [1]. In case (i), the mechanical interactions are enhanced by the hydrodynamic interactions, leading to $\phi_c(\sigma) < \phi_c^{(m)}(\sigma)$. In case (ii), both interactions are equally important, leading to $\phi_c(\sigma) = \phi_c^{(m)}(\sigma) = \phi_h(\sigma)$. In case (iii), the mechanical interactions are reduced by the hydrodynamic interactions, leading to $\phi_c(\sigma) > \phi_c^{(m)}(\sigma)$. In cases (i) and (iii), the hydrodynamic correlation effects dominate the system, leading to $\phi_c(\sigma) = \phi_h(\sigma)$. Here we note that only in case (ii) the simulation results can describe the experimental data. Since the TMCT equation with the hydrodynamic memory function cannot be solved analytically nor numerically at the present moment, we just demonstrate from a phenomenological point of view based on the theoretical prediction how one can qualitatively explain the three cases consistently. In order to check the existence of those three cases, therefore, we investigate not only the polydispersity dependence of the critical point obtained from the experiments for suspensions of polydisperse hard-sphere colloids [4,5,7–11] but also that of the simulations [28–36]. Then, we show on a schematic representation of the phase diagram in volume fraction-polydispersity plane that the polydispersity dependence of the experimental critical point $\phi_c(\sigma)$ coincides with Eq. (2) within error and is quite different from that of the simulations given by $\phi_c^{(m)}(\sigma)$. Thus, we emphasize that the hydrodynamic interactions are indispensable to explain the experimental results for the suspensions of polydisperse hard-sphere colloids.

We begin in Section 2 by briefly explaining the theoretical background of TMCT. Then, we derive the TMCT equation for colloidal suspensions, starting from the nonlinear Markov Langevin equations with the friction coefficient resulted from the long-range hydrodynamic interactions between colloids. In Section 3, we investigate the nonlinear memory function in TMCT equation, which contains two different correlation effects; one due to the mechanical interactions and the other due to the hydrodynamic interactions. In Section 4, we discuss the ergodic to non-ergodic transition at a critical point and derive a nonlinear equation to find a Debye–Waller factor. In Section 5, we propose an asymptotic form of the friction coefficient to obtain three cases qualitatively. In Section 6, we investigate the critical volume fractions obtained from the experiments and the simulations for the suspensions of polydisperse hard-sphere colloids. Thus, we show the phase diagram in volume fraction-polydispersity plane and discuss how the hydrodynamic interactions are indispensable to explain such a phase diagram qualitatively. We conclude in Section 7 with a summary.

2. TMCT for colloidal suspensions

In this section, we show how to apply the same TMCT formulation [44] as that employed in the molecular systems for colloidal suspensions. We consider the three-dimensional system which contains N spherical colloids with mass m_i and radius a_i of particle i suspended in an equilibrium fluid with a viscosity η in the total volume V at temperature T. Before we go into the details, we briefly review the theoretical background.

2.1. Theoretical background of TMCT

In this subsection, we briefly summarize the macroscopic equations in the suspensions which are derived from first principles by using a new formulation based on TMCT [44–47]. The outline of TMCT is as follows. As is shown in Fig. 1, the basic equations discussed in the present paper can be classified into four stages, [N], [L], [K], and [H], depending on a space–time scale. In a microscopic stage [N], the position $\boldsymbol{X}_j(t)$ and the momentum $\boldsymbol{P}_j(t)$ of jth particle at time t are described by the Newton (or Heisenberg) equations. In a Langevin stage [L], a nonlinear Langevin equation for the momentum $\boldsymbol{P}_j(t)$ is derived from the Newton equations. In a kinetic stage [K], the relevant variables are given by the current densities and the number densities. Linear non-Markov Langevin type equations for the current densities are derived from the Langevin equation by using the Mori projection-operator method [48] (see a dashed arrow (M) in Fig. 1), where the memory terms are convolution in time and are written in terms of correlation function of the fluctuating forces. Linear non-Markov stochastic

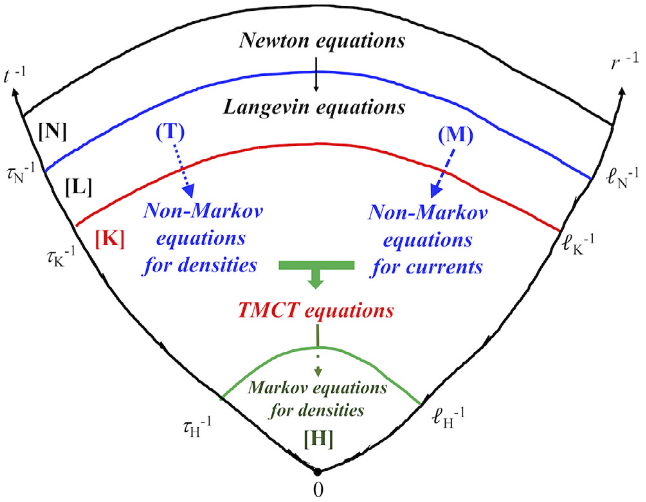

Fig. 1. (Color online) Classification of the basic equations discussed in the present paper into four stages, [N], [L], [K], and [H], depending on a space–time scale. Here ℓ_i and τ_i indicate the characteristic length and time, respectively.

diffusion equations for the number densities are also derived from the Langevin equation by employing the Tokuyama–Mori projection-operator method [49,50] (see a dotted arrow (T) in Fig. 1), where the memory terms are convolutionless in time and are written in terms of correlation function of the fluctuating current. Then, those coupled equations are used to obtain closed nonlinear non-Markov second-order differential equations for the average number densities (see a bold arrow in Fig. 1). This is a TMCT equation not only to describe the dynamics of supercooled liquids but also to find a critical point at which an ergodic to non-ergodic transition occurs. In a hydrodynamic stage [H], the Markov equations for number densities are derived (see a dot-dashed arrow in Fig. 1). As discussed in the previous papers [44–47], it is important to employ two types of projection-operator methods to derive the basic equations for different relevant variables. In fact, it is indispensable to use the time-convolutionless formalism for the number densities to recover the cumulant expansion proposed by Kubo [51]. Thus, TMCT enables us to calculate each cumulant-expansion term, such as a mean-square displacement and a non-Gaussian parameter, consistently from first principles.

2.2. A Langevin equation in stage [L]

Let $\{\boldsymbol{X}(t), \boldsymbol{P}(t)\}$ denote a set of variables, where $\boldsymbol{X}_i(t)$ and $\boldsymbol{P}_i(t)$ are the position vector and the momentum of the ith colloidal particle, respectively. As shown in the previous papers [19–21], there are three kinds of interactions acting on a colloidal particle i on a time scale of the Brownian relaxation time $t_B(= m_i/\zeta_{0i})$, where $\zeta_{0i} = 6\pi\eta a_i$. The first is a random force $\boldsymbol{R}_i(t)$ which is exerted by the fluctuating fluid on a colloid i, leading to Brownian motion. The second is hydrodynamic interactions between colloids i and j through the friction tensor $\boldsymbol{\zeta}_{ij}$. The last is mechanical interactions between colloids i and j given by $\boldsymbol{F}_{ij}(t)$, a force acting on the ith particle from the jth particle. Then, the colloidal particle is described by the nonlinear Markov Langevin equation, which can be derived from the Newton equation as [20,21]

$$\frac{d\boldsymbol{P}_i(t)}{dt} = -\sum_{j=1}^{N} \frac{\boldsymbol{\zeta}_{ij}(\boldsymbol{X}(t))}{m_j} \cdot \boldsymbol{P}_j(t) + \sum_{j\neq i}^{N} \boldsymbol{F}_{ij}(t) + \boldsymbol{R}_i(t), \tag{4}$$

where $\boldsymbol{R}_i(t)$ obeys a Gaussian, Markov process and satisfies the fluctuation–dissipation relation

$$\langle \boldsymbol{R}_i(t)\boldsymbol{R}_j(t'); \boldsymbol{x}, \boldsymbol{p}\rangle = 2k_BT\boldsymbol{\zeta}_{ij}(\boldsymbol{x})\delta(t-t'), \tag{5}$$

and the orthogonality condition $\langle \boldsymbol{R}_i(t); \boldsymbol{x}, \boldsymbol{p}\rangle = 0$. Here the brackets $\langle \cdots; \boldsymbol{x}, \boldsymbol{p}\rangle$ denote the conditional average over an equilibrium ensemble given by $\langle \cdots; \boldsymbol{x}, \boldsymbol{p}\rangle = \langle \cdots \Pi_{\boldsymbol{xp}}(0)\rangle/\langle \Pi_{\boldsymbol{xp}}(0)\rangle$, where $\Pi_{\boldsymbol{xp}}(t)$ is a generating function for $\{\boldsymbol{X}(t), \boldsymbol{P}(t)\}$ to have a set of variables $\{\boldsymbol{x}, \boldsymbol{p}\}$ and is given by $\Pi_{\boldsymbol{xp}}(t) = \prod_{i=1}^{N} \delta(\boldsymbol{X}_i(t)-\boldsymbol{x}_i)\delta(\boldsymbol{P}_i(t)-\boldsymbol{p}_i)$. The first term of Eq. (4) indicates the friction force. Here the friction tensor $\boldsymbol{\zeta}_{ij}(\boldsymbol{X}(t))$ depends on time only through $\boldsymbol{X}(t)$ and is given by

$$\boldsymbol{\zeta}_{ij}(\boldsymbol{x}) = \zeta_{0i}\left[(\mathbf{1}+\boldsymbol{G}(\boldsymbol{x}))^{-1}\right]_{ij}, \tag{6}$$

where the tensor $\boldsymbol{G}_{ij}(\boldsymbol{x})(i \neq j)$ indicates the hydrodynamic interactions between colloids i and j, and $\boldsymbol{G}_{ii} = 0$. Up to order $(a_i/|\boldsymbol{x}_{ij}|)^4$, the tensor $\boldsymbol{G}_{ij}$ can be written in terms of the Oseen tensor $\boldsymbol{G}_{ij}^O$ and the dipole tensor $\boldsymbol{G}_{ij}^D$ as $\boldsymbol{G}_{ij} = \boldsymbol{G}_{ij}^O + \boldsymbol{G}_{ij}^D$ with [19–21]

$$\boldsymbol{G}_{ij}^O = \frac{3}{4}\frac{a_i}{|\boldsymbol{x}_{ij}|}(\boldsymbol{1} + \hat{\boldsymbol{x}}_{ij}\hat{\boldsymbol{x}}_{ij}),$$
$$\boldsymbol{G}_{ij}^D = \frac{1}{4}\frac{a_i(a_i^2 + a_j^2)}{|\boldsymbol{x}_{ij}|^3}(\boldsymbol{1} - 3\hat{\boldsymbol{x}}_{ij}\hat{\boldsymbol{x}}_{ij}), \tag{7}$$

where $\hat{\boldsymbol{x}}_{ij} = \boldsymbol{x}_{ij}/|\boldsymbol{x}_{ij}|$, and $\boldsymbol{x}_{ij} = \boldsymbol{x}_i - \boldsymbol{x}_j$. Here we note that the explicit time dependence of ζ_{0i} caused by the back-flow effect as a long-time tail [52] is ignored for simplicity since it does not play any role in a diffusion process of interest. In the following, we deal with only identical particles with mass m and radius a for simplicity. Then, the control parameter is given by λ, such as a volume fraction $\phi(= 4\pi\rho a^3/3)$ in spherical colloids, inverse temperature $1/T$ in Lennard-Jones colloids, etc., where $\rho(= N/V)$ is the number density.

Eq. (4) is a starting equation to derive stochastic equations in stages [K] and [H]. As discussed in the previous papers [44–47], in the molecular systems one can easily derive such equations by employing the projection operator method [48–50]. This is because the position vector $\boldsymbol{X}_i(t)$ and the momentum $\boldsymbol{P}_i(t)$ are described by the Heisenberg equations with the Liouville operator L. On the other hand, in the colloidal suspensions $\boldsymbol{P}_i(t)$ obeys the Langevin equation (4). In order to directly apply the same projection operator method as that used in the molecular systems to the colloidal systems, therefore, it is convenient to start from a stochastic Fokker–Planck equation for $\Pi_{\boldsymbol{xp}}(t)$ as discussed in the previous papers [53,54]. Let $A_q(\boldsymbol{X}(t), \boldsymbol{P}(t))$ be an arbitrary function of $\{\boldsymbol{X}(t), \boldsymbol{P}(t)\}$. Then, one can write it as $A_q(\boldsymbol{X}(t), \boldsymbol{P}(t)) = \int d\boldsymbol{x} \int d\boldsymbol{p} A_q(\boldsymbol{x}, \boldsymbol{p})\Pi_{\boldsymbol{xp}}(t)$. As is shown in Appendix, therefore, the function $A_q(\boldsymbol{x}, \boldsymbol{p}, t)$ can be described by a new equation

$$\frac{\partial}{\partial t}A_q(\boldsymbol{x}, \boldsymbol{p}, t) = \Lambda(\boldsymbol{x}, \boldsymbol{p})A_q(\boldsymbol{x}, \boldsymbol{p}, t) \tag{8}$$

with the operator

$$\Lambda(\boldsymbol{x}, \boldsymbol{p}) = \sum_{i=1}^{N}\left[\frac{\boldsymbol{p}_i}{m}\cdot\frac{\partial}{\partial \boldsymbol{x}_i} + \frac{\partial}{\partial \boldsymbol{p}_i}\cdot\sum_{j\neq i}^{N}\boldsymbol{F}_{ij}\right]$$
$$+ \sum_{i=1}^{N}\sum_{j=1}^{N}\left[-\frac{1}{m}\boldsymbol{p}_i + k_BT\frac{\partial}{\partial \boldsymbol{p}_i}\right]\cdot\boldsymbol{\zeta}_{ij}\cdot\frac{\partial}{\partial \boldsymbol{p}_j}. \tag{9}$$

This equation plays a role of the Heisenberg equation in the colloidal systems. In fact, Eq. (8) is formally solve to give $A_q(\boldsymbol{x}, \boldsymbol{p}, t) = \exp[t\Lambda(\boldsymbol{x}, \boldsymbol{p})]A_q(\boldsymbol{x}, \boldsymbol{p})$. Thus, it turns out that one can directly apply the same TMCT formulation as that discussed in molecular systems to colloidal suspensions, except that the operator iL is now replaced by Λ. We next discuss this briefly.

2.3. An equation for $f(q, t)$ in stage [K]

We first discuss the macroscopic equation in a stage [K]. In this paper, we focus only on the dynamics of collective-intermediate scattering function given by

$$f(q, t) = \langle\rho(\boldsymbol{q}, \boldsymbol{X}(t))\rho(\boldsymbol{q}, \boldsymbol{X}(0))^*\rangle/S(q) \tag{10}$$

with the colloid density fluctuation

$$\rho(\boldsymbol{q}, \boldsymbol{X}(t)) = \frac{1}{N^{1/2}}\left[\sum_{j=1}^{N}e^{i\boldsymbol{q}\cdot\boldsymbol{X}_j(t)} - N\delta_{\boldsymbol{q},0}\right], \tag{11}$$

where $S(q)(= \langle|\rho(\boldsymbol{q}, \boldsymbol{X}(0))|^2\rangle)$ is a static structure factor and $q = |\boldsymbol{q}|$. Since the density fluctuation is a macroscopic quantity, we set q as $0 < q \leq q_c$, where q_c is a wave number cutoff to be determined. As is shown in Eq. (A.8), one can then write $f(q, t)$ as

$$f(q, t) = \langle\rho(\boldsymbol{q}, \boldsymbol{x}(t))\rho(\boldsymbol{q}, \boldsymbol{x}(0))^*\rangle/S(q), \tag{12}$$

where $\rho(\boldsymbol{q}, \boldsymbol{x}(t)) = \exp[t\Lambda(\boldsymbol{x}, \boldsymbol{p})]\rho(\boldsymbol{q}, \boldsymbol{x})$. By simply writing $\rho(\boldsymbol{q}, \boldsymbol{x}(t))$ as $\rho(\boldsymbol{q}, t)$, the starting equation is now given by

$$\frac{\partial}{\partial t}\rho(\boldsymbol{q}, t) = \Lambda(\boldsymbol{x}, \boldsymbol{p})\rho(\boldsymbol{q}, t). \tag{13}$$

Similarly to the molecular systems, we also introduce the projection operator $\wp$ by

$$\wp A(t) = \frac{\langle A(t)\rho(\boldsymbol{q}, 0)^*\rangle}{\langle\rho(\boldsymbol{q}, 0)\rho(\boldsymbol{q}, 0)^*\rangle}\rho(\boldsymbol{q}, 0). \tag{14}$$

By using the time-convolutionless projection-operator method (T) [49,50], one can then exactly transform Eq. (13) into a time-convolutionless linear stochastic diffusion equation for $\rho(\boldsymbol{q},t)$

$$\frac{\partial}{\partial t}\rho(\boldsymbol{q},t)=-q^2D_c(q,t)\rho(\boldsymbol{q},t)+iqg(\boldsymbol{q},t) \tag{15}$$

with the time- and q-dependent collective-diffusion coefficient

$$D_c(q,t)=\int_0^t\psi(q,s)ds, \tag{16}$$

where the memory function $\psi(q,t)$ is given by

$$\psi(q,t)=\langle g(\boldsymbol{q},t)g(\boldsymbol{q},0)^*\rangle/\langle\rho(\boldsymbol{q},t)\rho(\boldsymbol{q},0)^*\rangle. \tag{17}$$

Here $g(\boldsymbol{q},t)$ is a fluctuating current given by

$$g(\boldsymbol{q},t)=e^{tQ\Lambda}[1-Q\{1-e^{-t\Lambda}e^{tQ\Lambda}\}]^{-1}j(\boldsymbol{q},0) \tag{18}$$

with the current density fluctuation

$$j(\boldsymbol{q},0)=N^{-1/2}\sum_{j=1}^{N}\hat{\boldsymbol{q}}\cdot\frac{\boldsymbol{p}_j}{m}e^{i\boldsymbol{q}\cdot\boldsymbol{x}_j}, \tag{19}$$

where $Q=1-\wp$ and $\hat{\boldsymbol{q}}=\boldsymbol{q}/|\boldsymbol{q}|$. The fluctuating current $g(\boldsymbol{q},t)$ satisfies the orthogonality condition given by $\langle g(\boldsymbol{q},t)\rho(\boldsymbol{q},0)^*\rangle=0$. Here we have $\langle|g(\boldsymbol{q},0)|^2\rangle=v_{th}^2(=k_BT/m)$, $\psi(q,0)=v_{th}^2/S(q)$, and $D_c(q,0)=0$. Use of Eqs. (12) and (15) then leads to a time-convolutionless diffusion equation for $f(q,t)$

$$\frac{\partial}{\partial t}f(q,t)=-q^2D_c(q,t)f(q,t). \tag{20}$$

This equation is easily solved to find a formal solution

$$f(q,t)=\exp[-K(q,t)] \tag{21}$$

with the cumulant function

$$K(q,t)=q^2\int_0^t D_c(q,s)ds=q^2\int_0^t(t-s)\psi(q,s)ds, \tag{22}$$

where $K(q,0)=dK(q,t)/dt|_{t=0}=0$.

2.4. An equation for $\psi(q,t)$ in stage [K]

We next derive the equation for $\psi(q,t)$ in a stage [K]. As discussed in Refs. [44,47], one can write a time derivative of Eq. (18) as

$$\frac{\partial}{\partial t}g(\boldsymbol{q},t)=Q\Lambda g(\boldsymbol{q},t)-iq\psi(q,t)Q\rho(\boldsymbol{q},t)\simeq Q\Lambda g(\boldsymbol{q},t). \tag{23}$$

In order to derive Eq. (23), we have used the fact that $\psi(q,t)\rho(\boldsymbol{q},t)\simeq\psi(q,t)\rho(\boldsymbol{q},0)$ since $\psi(q,t)$ is a rapidly-varying function in time, while $\rho(\boldsymbol{q},t)$ is a slowly-varying function in time [44]. Because of the same reason, one can also write Eq. (17) approximately as

$$\psi(q,t)\simeq\langle g(\boldsymbol{q},t)g(\boldsymbol{q},0)^*\rangle/S(q). \tag{24}$$

Here we note that although a precise formulation without this approximation has been recently done in Ref. [47], we can safely use Eq. (24) in the following because we are interested only in the long-time dynamics near the critical point.

In order to derive a linear equation for $\psi(q,t)$ from Eq. (23), we also introduce the projection operator $\wp'$ by

$$\wp'A(t)=\frac{\langle A(t)g(\boldsymbol{q},0)^*\rangle}{\langle g(\boldsymbol{q},0)g(\boldsymbol{q},0)^*\rangle}g(\boldsymbol{q},0). \tag{25}$$

Similarly to the molecular systems, one can use the time-convolution projection-operator method [48] to derive a linear Langevin type equation for $g(\boldsymbol{q},t)$. Then, one can exactly transform Eq. (23) into

$$\frac{\partial}{\partial t}g(\boldsymbol{q},t)=i\omega g(\boldsymbol{q},t)-\int_0^t\Delta\varphi(q,s)g(\boldsymbol{q},t-s)ds+\xi(\boldsymbol{q},t) \tag{26}$$

with the drift term

$$i\omega=\langle[Q\Lambda g(\boldsymbol{q},0)]g(\boldsymbol{q},0)^*\rangle/v_{th}^2=-\zeta(q)/m, \tag{27}$$

and the nonlinear memory term

$$\Delta\varphi(q,t)=-\langle[Q\Lambda\xi(\boldsymbol{q},t)]g(\boldsymbol{q},0)^*\rangle/v_{th}^2=\langle\xi(\boldsymbol{q},t)\xi(\boldsymbol{q},0)^*\rangle/v_{th}^2, \tag{28}$$

where the friction coefficient $\zeta(q)$ is given by

$$\zeta(q)=\frac{1}{N}\sum_{i=1}^{N}\sum_{j=1}^{N}\langle\hat{\boldsymbol{q}}\cdot\boldsymbol{\zeta}_{ij}\cdot\hat{\boldsymbol{q}}e^{i\boldsymbol{q}\cdot\boldsymbol{x}_{ij}}\rangle. \tag{29}$$

Here $\xi(\boldsymbol{q},t)$ is the fluctuating force given by

$$\xi(\boldsymbol{q},t)=e^{tQ'Q\Lambda}Q'Q\Lambda g(\boldsymbol{q},0), \tag{30}$$

and satisfies the orthogonality conditions $\langle\xi(\boldsymbol{q},t)g(\boldsymbol{q},0)^*\rangle=\langle\xi(\boldsymbol{q},t)\rho(\boldsymbol{q},0)^*\rangle=0$, where $Q'=1-\wp'$. Use of Eqs. (24) and (26) then leads to

$$\frac{\partial}{\partial t}\psi(q,t)=-\frac{\zeta(q)}{m}\psi(q,t)-\int_0^t\Delta\varphi(q,s)\psi(q,t-s)ds. \tag{31}$$

This is a linear non-Markov equation for $\psi(q,t)$ whose memory function is convolution in time.

2.5. A second-order differential equation for $K(q,t)$ in stage [K]

In order to find $f(q,t)$, one has to solve the coupled equations given by Eqs. (20) and (31) consistently. However, one can transform those equations into a single equation for $K(q,t)$ [45]. In fact, this is easily done by introducing the Laplace transform of $K(q,t)$ by $K[q,z]=\int_0^\infty e^{-zt}K(q,t)dt$. By taking the Laplace transform of Eq. (31) and using the relation $\psi[q,z]=z^2K[q,z]$, we thus obtain the second-order differential equation for $K(q,t)$

$$\frac{\partial^2K(q,t)}{\partial t^2}=\frac{q^2v_{th}^2}{S(q)}-\frac{\zeta(q)}{m}\frac{\partial K(q,t)}{\partial t}-\int_0^t\Delta\varphi(q,t-s)\frac{\partial K(q,s)}{\partial s}ds. \tag{32}$$

This equation has exactly the same form as that obtained in the molecular systems [45], except that the damping constant is now replaced by $\zeta(q)/m$. On a time scale of a structural relaxation time $t_D(=a^2/D_0)$ much longer than t_B, one can safely neglect the second derivative term in Eq. (32) and finally obtain

$$\frac{\partial K(q,t)}{\partial t}=q^2D_c^S(q)-\frac{m}{\zeta(q)}\int_0^t\Delta\varphi(q,t-s)\frac{\partial K(q,s)}{\partial s}ds, \tag{33}$$

where $D_c^S(q)(=D_0\zeta_0/S(q)\zeta(q))$ is the q-dependent short-time collective diffusion coefficient resulted from the hydrodynamic interactions, $D_0(=k_BT/\zeta_0)$ being a single particle diffusion constant. This is the TMCT equation to discuss the dynamics of colloidal suspensions on a time scale of t_D. Here we note that all the assumptions and formulations used here are the same as those employed in TMCT in the molecular systems. Only the difference between the molecular systems and colloidal suspensions appears in the nonlinear memory function $\Delta\varphi(\boldsymbol{q},t)$. We next discuss this.

2.6. A Markov equation for $K(q,t)$ in stage [H]

On a time scale much longer than t_D, Eq. (33) reduces to a Markov equation

$$\begin{aligned}\frac{\partial K(q,t)}{\partial t}&\simeq q^2D_c^S(q)-\frac{m}{\zeta(q)}\int_0^\infty\Delta\varphi(q,s)ds\frac{\partial K(q,t)}{\partial t}\\&=q^2D_c^L(q)\end{aligned} \tag{34}$$

with the wavevector-dependent long-time collective diffusion coefficient $D_c^L(q)$

$$D_c^L(q)=D_c(q,\infty)=\frac{D_c^S(q)}{1+S(q)D_c^S(q)\int_0^\infty ds\Delta\varphi(q,s)/v_{th}^2}. \tag{35}$$

Then, this leads to

$$K(q,t)=q^2D_c^L(q)t. \tag{36}$$

3. Nonlinear memory function

In colloidal suspensions, the fluctuating force $\xi(\boldsymbol{q},t)$ consists of two types of interactions. One is a mechanical interaction between particles i and j due to the force $\boldsymbol{F}_{ij}$ and the other is a hydrodynamic interaction between i and j through the friction force $-\boldsymbol{\zeta}_{ij}\cdot\mathbf{p}_j/m$. In order to take into account the nonlinear effects from both interactions, we now introduce a new projection operator $\wp_2$ by

$$\begin{aligned}\wp_2 A =& \sum_{|\mathbf{k}|\le q_c}\left[\frac{\langle A\rho(\mathbf{k},0)^*\rho(\mathbf{q}-\mathbf{k},0)^*\rangle}{2S(k)S(|\mathbf{q}-\mathbf{k}|)}\rho(\mathbf{k},0)\rho(\mathbf{q}-\mathbf{k},0)\right.\\ &+\frac{\langle Aj(\mathbf{k},0)^*\rho(\mathbf{q}-\mathbf{k},0)^*\rangle}{v_{th}^2S(|\mathbf{q}-\mathbf{k}|)}j(\mathbf{k},0)\rho(\mathbf{q}-\mathbf{k},0)\\ &\left.+\frac{\langle A\varepsilon(\mathbf{k},0)^*\rho(\mathbf{q}-\mathbf{k},0)^*\rangle}{2v_{th}^4S(|\mathbf{q}-\mathbf{k}|)}\varepsilon(\mathbf{k},0)\rho(\mathbf{q}-\mathbf{k},0)\right]\end{aligned}\tag{37}$$

with the kinetic energy density fluctuation

$$\varepsilon(\mathbf{k},0)=N^{-1/2}\sum_{j=1}^{N}\left[\left(\hat{\mathbf{k}}\cdot\frac{\mathbf{p}_j}{m}\right)^2-v_{th}^2\right]e^{i\mathbf{k}\cdot\mathbf{x}_j},\tag{38}$$

where $\wp_2(1-\wp_2)A=0$ because of the orthogonality conditions

$$\langle j(\mathbf{k},0)\rho(\mathbf{k},0)^*\rangle=\langle\varepsilon(\mathbf{k},0)\rho(\mathbf{k},0)^*\rangle=\langle j(\mathbf{k},0)\varepsilon(\mathbf{k},0)^*\rangle=0.\tag{39}$$

The first term of Eq. (37) is the same nonlinear term as that discussed in the mode-coupling theory (MCT) [55]. The second and third terms are new nonlinear terms, which are important to take into account the correlation effects due to the long-range hydrodynamic interactions. By using $\wp_2$, one can formally split the fluctuating force $\xi(\mathbf{q},t)$ into two parts as

$$\xi(\mathbf{q},t)=e^{tQ'Q\Lambda}\wp_2[Q'Q\Lambda j(\mathbf{q})]+e^{tQ'Q\Lambda}Q_2[Q'Q\Lambda j(\mathbf{q})],\tag{40}$$

where $Q_2=1-\wp_2$. Since the fluctuating force $\xi(\mathbf{q},t)$ does not contain the random motion which has been already extracted in Eq. (4) as the friction term, the second term of Eq. (40) contains the higher than third-order terms in $\rho(\mathbf{k},t)$, which are of order N^{-1}. Hence one can neglect it safely in the thermodynamic limit $N\to\infty$ and $V\to\infty$ with ρ being kept constant. By using Eq. (37), one can then write $\xi(\mathbf{q},t)$ as

$$\begin{aligned}\xi(\mathbf{q},t)\simeq& e^{tQ'Q\Lambda}\wp_2[Q'Q\Lambda j(\mathbf{q})]\\ =&\frac{1}{N^{1/2}}\sum_{|\mathbf{k}|\le q_c}\left[i\frac{v_{th}^2}{2}\rho v(\mathbf{q},\mathbf{k})\tilde{\rho}(\mathbf{k},t)\tilde{\rho}(\mathbf{q}-\mathbf{k},t)\right.\\ &\left.+\frac{v_{th}^2}{kD_0}u(\mathbf{q},\mathbf{k})\tilde{j}(\mathbf{k},t)\tilde{\rho}(\mathbf{q}-\mathbf{k},t)+iw(\mathbf{q},\mathbf{k})\tilde{\varepsilon}(\mathbf{k},t)\tilde{\rho}(\mathbf{q}-\mathbf{k},t)\right]\end{aligned}\tag{41}$$

with the vertexes

$$v(\mathbf{q},\mathbf{k})=\hat{\mathbf{q}}\cdot\mathbf{k}c(k)+\hat{\mathbf{q}}\cdot(\mathbf{q}-\mathbf{k})c(|\mathbf{q}-\mathbf{k}|),\tag{42}$$

$$u(\mathbf{q},\mathbf{k})=\hat{\mathbf{q}}\cdot[\zeta(q)\mathbf{1}-\boldsymbol{\zeta}(\mathbf{q},\mathbf{k})]\cdot\mathbf{k}/\zeta_0,\tag{43}$$

$$w(\mathbf{q},\mathbf{k})=\hat{\mathbf{q}}\cdot\mathbf{k},\tag{44}$$

where $\tilde{A}(\mathbf{k},t)=e^{tQ'Q\Lambda}A(\mathbf{k},0)$, and $\rho c(k)=1-1/S(k)$. Here $\boldsymbol{\zeta}(\mathbf{q},\mathbf{k})$ is a friction tensor given by

$$\boldsymbol{\zeta}(\mathbf{q},\mathbf{k})=\sum_{i,j}^{N}\frac{\langle\boldsymbol{\zeta}_{ij}e^{i\mathbf{q}\cdot\mathbf{x}_i-i\mathbf{k}\cdot\mathbf{x}_j}\rho(\mathbf{q}-\mathbf{k})^*\rangle}{N^{1/2}S(|\mathbf{q}-\mathbf{k}|)},\tag{45}$$

where we have approximated the time evolution of $\tilde{A}(\mathbf{k},t)$ as $\tilde{A}(\mathbf{k},t)\simeq A(\mathbf{k},t)$ [44,55]. By using the factorization approximation for $\langle\xi(\mathbf{q},t)\xi(\mathbf{q},0)^*\rangle$, from Eqs. (28), (39) and (41), one can thus write the nonlinear memory function $\Delta\varphi(q,t)$ as

$$\Delta\varphi(q,t)=\Delta\varphi_m(q,t)+\Delta\varphi_h(q,t)\tag{46}$$

with the mechanical memory function

$$\Delta\varphi_m(q,t)=\frac{\rho v_{th}^2}{2}\int_<\frac{d\mathbf{k}}{(2\pi)^3}v(\mathbf{q},\mathbf{k})^2S(k)S(|\mathbf{q}-\mathbf{k}|)f(k,t)f(|\mathbf{q}-\mathbf{k}|,t),\tag{47}$$

and the hydrodynamic memory function

$$\Delta\varphi_h(q,t)=\frac{v_{th}^2}{\rho}\int_<\frac{d\mathbf{k}}{(2\pi)^3}\left[w(\mathbf{q},\mathbf{k})^2-\chi(\mathbf{q},\mathbf{k},t)^2\right]S(k)S(|\mathbf{q}-\mathbf{k}|)f(k,t)f(|\mathbf{q}-\mathbf{k}|,t),\tag{48}$$

where the friction term $\chi(\boldsymbol{q}, \boldsymbol{k}, t)$ is given by

$$\chi(\boldsymbol{q}, \boldsymbol{k}, t) = u(\boldsymbol{q}, \boldsymbol{k})\frac{D_c(k, t)}{D_0}. \tag{49}$$

Here $\int_<$ denotes the sum over wave vectors $\boldsymbol{k}$ with $|\boldsymbol{k}| \leq q_c$. The memory function $\Delta\varphi_m(q, t)$ has the same form as that originally obtained in molecular systems [44,55]. The memory function $\Delta\varphi_h(q, t)$ is a new term resulted from the hydrodynamic effects, which consists of the coupling between the current densities and also that between the energy densities. In order to find the asymptotic form of $\varepsilon(\boldsymbol{k}, t)$ on a time scale of order τ_D, we have used the same formulation as that employed in the derivation of Eq. (4.2c) for the average number density in Ref. [21] and then obtained $\varepsilon(\boldsymbol{k}, t) \simeq v_{th}^2\rho(\boldsymbol{k}, t)$ from Eq. (3.49c) for the density fluctuation in Ref. [21]. Finally, we also note that the term which contains the short-time function $\psi(k, t)$ is neglected in Eq. (48) because it reduces to zero on a time scale of t_D.

4. Ergodic to non-ergodic transition

The most important prediction of MCT [55] is an existence of ergodic to non-ergodic transition at a critical point λ_c, such as a critical volume fraction ϕ_c, above which the long-time solution reduces to a non-zero value, the so-called Debye–Waller factor $f(q)$. This prediction has been also shown to hold for TMCT [44–47,56–58]. Taking the Laplace transform of Eq. (32), one can obtain

$$f(q) = \lim_{t\to\infty} f(q, t) = \begin{cases} 0, & \text{for } \lambda < \lambda_c, \\ \exp[-K(q)], & \text{for } \lambda \geq \lambda_c \end{cases} \tag{50}$$

with the long-time cumulant function

$$K(q) = \lim_{z\to 0} zK[q, z] = 1/\mathcal{F}(q), \tag{51}$$

where the long-time limit of the memory function $\mathcal{F}(q)$ is given by

$$\mathcal{F}(q) = \lim_{z\to 0} \frac{z\Delta\varphi[\boldsymbol{q}, z]S(q)}{q^2 v_{th}^2} = \mathcal{F}_m(q) + \mathcal{F}_h(q). \tag{52}$$

Here the mechanical memory term $\mathcal{F}_m(q)$ and the hydrodynamic memory term $\mathcal{F}_h(q)$ are given by

$$\mathcal{F}_m(q) = \frac{\rho}{2q^2}\int_< \frac{d\boldsymbol{k}}{(2\pi)^3} v(\boldsymbol{q}, \boldsymbol{k})^2 S(q)S(k)S(|\boldsymbol{q} - \boldsymbol{k}|)f(k)f(|\boldsymbol{q} - \boldsymbol{k}|), \tag{53}$$

$$\mathcal{F}_h(q) = \frac{1}{\rho q^2}\int_< \frac{d\boldsymbol{k}}{(2\pi)^3} \Omega(\boldsymbol{q}, \boldsymbol{k})S(q)S(k)S(|\boldsymbol{q} - \boldsymbol{k}|)f(k)f(|\boldsymbol{q} - \boldsymbol{k}|), \tag{54}$$

where the hydrodynamic vertex Ω is given by

$$\Omega(\boldsymbol{q}, \boldsymbol{k}) = w(\boldsymbol{q}, \boldsymbol{k})^2 - \chi(\boldsymbol{q}, \boldsymbol{k}, \infty)^2. \tag{55}$$

From Eqs. (50) and (51), one obtains

$$f(q) = \exp[-1/\mathcal{F}(q)], \quad \text{or} \quad K(q)\mathcal{F}(q) = 1. \tag{56}$$

This is an equation to find the Debye–Waller factor $f(q)$ or the nonergodicity cumulant $K(q)$. Since $\mathcal{F}(q)$ contains the nonlinear terms $\exp[-K(k) - K(|\boldsymbol{q} - \boldsymbol{k}|)]$, the function $K(q)$ is considered to be a kind of the so-called Lambert W-function, which ensures the existence of a critical point mathematically. We should mention here that the critical point λ_c is just a mathematical singular point but not the thermodynamic glass transition point λ_g, where $\lambda_c > \lambda_g$. Here we note that Eq. (56) has the same form as that obtained in the molecular systems, except that the memory function contains the hydrodynamic term. If the hydrodynamic term is neglected, therefore, the critical point obtained in suspensions of hard spheres coincides with that in the hard-sphere fluids. This has been already checked between the Brownian-dynamics simulations and the molecular-dynamics simulations [29,30].

The second important prediction of MCT is that there exists a two-step relaxation process in a β stage. As demonstrated in Refs. [45,56], one can directly apply exactly the same formulation as that employed by MCT to TMCT near λ_c. Near λ_c, therefore, one can write the α-relaxation time τ_α and the β-relaxation time τ_β as

$$\tau_\alpha \propto (1 - \lambda/\lambda_c)^{-\gamma}, \tag{57}$$

$$\tau_\beta \propto (1 - \lambda/\lambda_c)^{-\gamma_\beta}, \tag{58}$$

where γ and γ_β are time exponents to be determined. In stage [H], we obtain

$$K(q, t) \simeq \begin{cases} q^2 D_c^L(q)t, & \text{for } \lambda < \lambda_c, \\ K(q), & \text{for } \lambda \geq \lambda_c. \end{cases} \tag{59}$$

Since $\tau_\alpha \propto 1/D_c^L$, one can also write $D_c^L(q)$ near λ_c as

$$D_c^L(q) \propto (1-\lambda/\lambda_c)^\gamma. \tag{60}$$

From Eq. (35), the integral term of $\Delta\varphi(q,s)$ is thus expected to be a singular function proportional to τ_α. Here we note that the self-diffusion coefficient D_s^L also obeys the same power law as that of Eq. (60), except that γ is now replaced by γ_s.

If $\mathcal{F}_h(q)$ is neglected, Eq. (56) is exactly the same equation as that in the molecular systems [44–47] and leads to a mechanical critical point $\lambda_c^{(m)}$. Depending on a sign of $\mathcal{F}_h(q)$, therefore, we may have the following three cases for the critical point λ_c. The first is a case (i) where $\mathcal{F}_h(q) > 0$. From Eq. (56), one thus finds that $\lambda_c < \lambda_c^{(m)}$ since the mechanical interactions are enhanced by the long-range hydrodynamic interactions. The second is a case (ii) where $\mathcal{F}_h(q) = 0$. Then, one finds that $\lambda_c = \lambda_c^{(m)}$. This suggests that the dynamics in the experiments can be described by the Brownian-dynamics (BD) simulations. The last is a case (iii) where $\mathcal{F}_h(q) < 0$. Then, one finds that $\lambda_c > \lambda_c^{(m)}$ since the mechanical interactions are reduced by the long-range hydrodynamic interactions. In the next section, we discuss whether those three cases are possible in the experiments for suspensions of hard-sphere colloids or not.

5. Hydrodynamic interactions in suspensions of polydisperse hard spheres

In order to discuss how the hydrodynamic interactions between particles play an important role near the critical point, we consider the suspension of hard spheres with size polydispersity σ, where the control parameter λ is given by the volume fraction ϕ and the mechanical interactions are given by the direct interactions between colloids. We first mention that because of the vertex $u(\boldsymbol{q},\boldsymbol{k})$, it is not easy to find the critical volume fraction $\phi_c(\sigma)$ by solving Eq. (56) even numerically. If the asymptotic form of u is given, however, $\phi_c(\sigma)$ is easily calculated at $\sigma = 0$ from Eq. (56) by using the Percus–Yevick (PY) static structure factor [59] (see Table 1). We next discuss such an asymptotic form from a phenomenological point of view and then show how one can qualitatively predict three cases discussed before.

5.1. Hydrodynamic singular point

In this subsection, we first discuss the hydrodynamic critical point $\phi_h(\sigma)$, which is obtained from the many-body correlation effects due to the long-range hydrodynamic interactions $\boldsymbol{G}_{ij}^O(i \neq j)$. The theoretical calculation of $\phi_h(\sigma)$ has been done only for monodisperse hard spheres, where $\sigma = 0$. As shown in Refs. [20,21], the long-time self-diffusion coefficient $D_s^{L(H)}(\phi)$ is calculated as

$$D_s^{L(H)}(\phi) = \frac{D_s^S(\phi)(1-9\phi/32)}{1+\frac{D_s^S(\phi)}{D_0}\frac{\phi/\phi_h(0)}{[1-\phi/\phi_h(0)]^2}}, \tag{61}$$

where the hydrodynamic critical point $\phi_h(0)$ is given by

$$\phi_h(0) = \frac{(4/3)^3}{7\ln(3) - 8\ln(2) + 2} \simeq 0.571847\cdots. \tag{62}$$

Here the factor $9\phi/32$ results from the coupling effects between the direct interactions and the short-range hydrodynamic interactions. The coefficient $D_s^S(\phi)$ is the short-time self-diffusion coefficient given by

$$D_s^S(\phi) = \frac{D_0}{1+H(\phi)}, \tag{63}$$

where $H(\phi)$ is the term resulted from the short-time hydrodynamic interactions and is given by [20]

$$H(\phi) = \hat{\boldsymbol{q}}\cdot\langle\boldsymbol{\zeta}_{ii}/\zeta_0\rangle\cdot\hat{\boldsymbol{q}} - 1, \tag{64}$$

$$\simeq \frac{9\phi/4}{1-(9\phi/8)^{1/2}} - \frac{11\phi/16}{1+11\phi/8} - \frac{(9\phi/8)^{1/2}(11\phi/16)(2+11\phi/16)}{(1+11\phi/16)(1-(9\phi/8)^{1/2}+11\phi/16)}. \tag{65}$$

The first term of Eq. (65) comes from the long-range hydrodynamic interactions, the second term from the short-range hydrodynamic interactions, and the third term from their couplings. Here we note that $D_s^{L(H)}$ is in general different from the long-time self-diffusion coefficient D_s^L because the singular point of the former is determined only by the hydrodynamic interaction, while that of the latter by both the mechanical interaction and the hydrodynamic interaction. Similarly to Eq. (61), the friction tensor $\boldsymbol{\zeta}_{ij}(i \neq j)$ is also calculated for a self-diffusion in monodisperse hard spheres as

$$\sum_{i(\neq j)}\langle\boldsymbol{\zeta}_{ij}\rangle/\zeta_0 \simeq \frac{\phi/\phi_h(0)}{[1-\phi/\phi_h(0)]^2}\mathbf{1}. \tag{66}$$

Here we note that the singular exponent and the singular point of Eq. (66) are the same as those of Eq. (61).

In order to extend Eqs. (61) and (66) to polydisperse hard spheres, one may replace a by $a+\delta a$ in those equations and average them over the Gaussian distribution function $P(\delta a) = \exp[-(\delta a)^2/(2\sigma^2 a^2)]/((2\pi)^{1/2}\sigma a)$ [1], where σ is a scaled standard deviation given by $\sigma = \langle(\delta a)^2\rangle^{1/2}/a$ and is assumed to be small. Up to lowest order in σ, one can thus obtain

$$D_s^{L(H)}(\phi) \propto D_0 \frac{[1-\phi/\phi_h(\sigma)]^2}{\phi/\phi_h(\sigma)}, \tag{67}$$

$$\sum_{i(\neq j)} \langle \boldsymbol{\zeta}_{ij} \rangle \simeq \zeta_0 \frac{\phi/\phi_h(\sigma)}{[1-\phi/\phi_h(\sigma)]^2} \mathbf{1}, \tag{68}$$

where $\phi_h(\sigma)$ is given by

$$\phi_h(\sigma) = (1+3\sigma^2)\phi_h(0). \tag{69}$$

Similarly to Eq. (43), one can also find the vertex u_s for a self-diffusion as

$$\begin{aligned} u_s(\boldsymbol{q},\boldsymbol{k}) &= -\hat{\boldsymbol{q}} \cdot \sum_{i(\neq j)} \langle \boldsymbol{\zeta}_{ij}/\zeta_0 e^{i\boldsymbol{k}\cdot\boldsymbol{x}_{ij}} \rangle \cdot \boldsymbol{k} \\ &\simeq -\frac{\phi/\phi_h(\sigma)}{[1-\phi/\phi_h(\sigma)]^2} \hat{\boldsymbol{q}} \cdot \boldsymbol{k} + O(k^2). \end{aligned} \tag{70}$$

Thus, the vertex u_s turns out to be a singular function with the hydrodynamic critical point $\phi_h(\sigma)$.

5.2. *Asymptotic form of hydrodynamic vertex $\Omega(\boldsymbol{q},\boldsymbol{k})$*

Since the vertex $u(\boldsymbol{q},\boldsymbol{k})$ contains the friction coefficient $\zeta(\boldsymbol{q},\boldsymbol{k})$ given by Eq. (45), it is not easy to obtain its singular function analytically. Hence we only discuss its asymptotic form here. Based on the discussion in Section 5.1, we now assume that the singular exponent of $u(\boldsymbol{q},\boldsymbol{k})$ is the same as that of $D_c^L(q)$ given by Eq. (60). Since the singular point of u is the same as that of u_s, one may assume the asymptotic form of u as

$$u(\boldsymbol{q},\boldsymbol{k}) \simeq -\frac{h(\sigma)}{[1-\phi/\phi_h(\sigma)]^\gamma} \hat{\boldsymbol{q}} \cdot \boldsymbol{k}, \tag{71}$$

where $h(\sigma)$ is a function of σ to be determined. Use of Eqs. (49), (60) and (71) then leads to

$$\chi(\boldsymbol{q},\boldsymbol{k},\infty;\phi) \simeq \begin{cases} -h(\sigma)\left[\frac{1-\phi/\phi_c}{1-\phi/\phi_h}\right]^\gamma \hat{\boldsymbol{q}}\cdot\boldsymbol{k}, & \text{for } \phi \le \phi_c, \\ 0, & \text{for } \phi > \phi_c. \end{cases} \tag{72}$$

At the critical point $\phi = \phi_c$, therefore, we obtain

$$\chi(\boldsymbol{q},\boldsymbol{k},\infty;\phi_c) = \begin{cases} -h(\sigma)\hat{\boldsymbol{q}}\cdot\boldsymbol{k}, & \text{for } \phi_c = \phi_h, \\ 0, & \text{for } \phi_c \neq \phi_h. \end{cases} \tag{73}$$

From Eq. (73), one can now explain the three cases discussed before consistently for hard-sphere colloids. We first mention that the case $\chi(\boldsymbol{q},\boldsymbol{k},\infty;\phi_c) = 0$ for $\phi_c \neq \phi_h$ does not exist because the memory function with vertex $w(\boldsymbol{q},\boldsymbol{k})$ leads to a unphysical critical volume fraction much lower than ϕ_h. When $\phi_c = \phi_h$, therefore, we find

$$\Omega(\boldsymbol{q},\boldsymbol{k},\sigma;\phi_c) = [1-h(\sigma)^2] w(\boldsymbol{q},\boldsymbol{k},\sigma;\phi_c)^2. \tag{74}$$

Then, there exist three cases; (i) $\Omega > 0$ (or $h < 1$), (ii) $\Omega = 0$ (or $h = 1$), and (iii) $\Omega < 0$ (or $h > 1$). When $\sigma = 0$, $h(0)$ can be determined from Eqs. (56) and (74) by using the PY static structure factor under the condition $\phi_c(0) = \phi_h(0)$. In fact, one can find $h(0) \simeq 0.9934$ at $q_c a = 14.5$. Since $h(0) < 1$, $\sigma = 0$ belongs to case (i). As σ increases, therefore, $h(\sigma)$ should increase and satisfy $h(\sigma_0) = 1$, where σ_0 is a non-zero value to be determined. Depending on the value of σ, we thus obtain the following three cases:

$$\begin{cases} \text{(i)} \;\; \phi_c(\sigma) = \phi_h(\sigma) < \phi_c^{(m)}(\sigma), & \text{for } 0 \le \sigma < \sigma_0, \\ \text{(ii)} \;\; \phi_c(\sigma) = \phi_h(\sigma) = \phi_c^{(m)}(\sigma), & \text{for } \sigma = \sigma_0, \\ \text{(iii)} \; \phi_c(\sigma) = \phi_h(\sigma) > \phi_c^{(m)}(\sigma), & \text{for } \sigma > \sigma_0. \end{cases} \tag{75}$$

Since $h \le 1$ in cases (i) and (ii), the condition $\mathcal{F}(q) > 0$ holds for all values of q. In case (iii), $h(\sigma)$ should also be a function of σ to satisfy such a condition.

6. Critical volume fraction for polydisperse hard-sphere colloids

In this section, we investigate the critical point obtained from the simulations and the experiments on suspensions of polydisperse hard-sphere colloids and also from the TMCT solutions for PY model. Then, we check whether there exist three cases discussed above or not. We note here that although the crystallization occurs above the melting volume fraction for $\sigma < 0.06$, one can safely find the critical volume fraction itself by using the power laws.

Table 1
$\phi_c(\sigma)$; (Exp.) experiments for hard spheres, (Sim.) simulations for hard spheres, and (TMCT) TMCT solution for PY model; (H0) without and (H) with hydrodynamic interactions, where $\sigma_0 \simeq 0.09545$.

σ	(Exp.)	$\phi_c(\sigma)$ (Sim.)	(TMCT)
0.00	–	0.582 [28–30]	(H0) 0.5817 [57] (H) 0.5718 (i)
0.04	(i) 0.575 [4,5]	–	–
0.05	(i) 0.577 ± 0.005 [6]	–	–
0.06	–	0.5845 [31]	–
0.069	(i) 0.580 [7,8]	–	–
0.07	–	0.5854 [33]	–
0.08	(i) 0.583 [9]	–	–
0.085	–	0.5865 [33]	–
σ_0	(ii)		–
0.10	(iii) 0.590 ± 0.005 [10]	0.5874 [35,36]	–
0.15	–	0.5919 [32]	–
0.23	–	0.598 [34]	–

6.1. Critical point obtained from simulations

By using the power laws given by Eqs. (57) and (60), the critical point $\phi_c(\sigma)$ has been found from the simulation results not only for the long-time self-diffusion coefficient D_S^L at $\sigma = 0.0, 0.06, 0.15$ [28–32], $\sigma = 0.07$ and 0.085 [33], and $\sigma = 0.23$ [34] but also for the α-relaxation time τ_α of the self-intermediate scattering function at $\sigma = 0.10$ [35,36]. The critical points at different polydispersities are listed in Table 1.

6.2. Critical point obtained from TMCT equation

In this subsection, we briefly refer to the critical point $\phi_c(0)$ obtained by solving Eq. (56) numerically at $\sigma = 0$ under the PY static structure factor. When $\mathcal{F}_h(q) = 0$, the critical point has been found as $\phi_c^{(m)}(0) \simeq 0.5817$ [57], which coincides with that of the simulations [28–30]. As discussed in Section 5.2, when $\mathcal{F}_h(q) \neq 0$, the critical point is found as $\phi_c(0) = \phi_h(0)$ at $h(0) \simeq 0.9934$.

6.3. Critical point obtained from experiments

By using the power laws given by Eqs. (57) and (60), the critical point $\phi_c(\sigma)$ has been reported from the following five different experiments for suspensions of hard-sphere colloids at different polydispersities. The first experiment has been done by van Megen et al. [4,5] at $\sigma \simeq 0.04$, where the critical point has been found as $\phi_c(0.04) \simeq 0.575$. The second one has been done by Phan et al. [6] at $\sigma \simeq 0.05$, where the critical point has been found as $\phi_c(0.05) \simeq 0.577 \pm 0.005$ by using the Krieger–Dougherty equation. The third one has been done by Pham et al. [7,8] at $\sigma \simeq 0.069$, where the critical point has been found as $\phi_c(0.069) \simeq 0.580$. The fourth one has been done by Kasper et al. [9] at $\sigma \simeq 0.08$, where the critical point has been found as $\phi_c(0.08) \simeq 0.583$. All those experiments belong to case (i) since $\phi_c(\sigma) \simeq \phi_h(\sigma) < \phi_c^{(m)}(\sigma)$. The last one has been done by Brambilla, et al. [10] at $\sigma \simeq 0.1$, where the critical volume fraction has been found as $\phi_c(0.1) \simeq 0.590 \pm 0.005$. Since $\phi_c(0.1) \simeq \phi_h(0.1) > \phi_c^{(m)}(0.1)$, this experiment belongs to case (iii). All the critical points are listed in Table 1. Finally, we refer to a possibility of case (ii). The simulation results are approximately described by the simulation line given by

$$\phi_c^{(m)}(\sigma) = 0.57971 + 0.079786\sigma, \quad \text{for } \sigma \geq 0.06. \tag{76}$$

Hence the point of intersection of it with the hydrodynamic critical point $\phi_h(\sigma)$ is found to be $\sigma_0 \simeq 0.094866$ at $\phi_h(\sigma_0) = 0.58728$. If the simulations and the experiments are done at $\sigma = \sigma_0$, therefore, both results are expected to coincide with each other.

6.4. Phase diagram

In Fig. 2, the schematic representation of the phase diagram in volume fraction-polydispersity plane is shown, where the detailed values of $\phi_c(\sigma)$ are listed in Table 1. We note here that the critical points of the experiments coincide with the hydrodynamic critical points $\phi_h(\sigma)$ given by Eq. (69) within error and are very sensitive to a polydispersity σ. On the other hand, those of the simulations obey Eq. (76) and are not so sensitive to σ [33]. This difference cannot be explained without the long-range hydrodynamic interactions since all the simulations for hard spheres are performed only under direct interactions without them. Thus, the experimental results may support the asymptotic form of $u(\boldsymbol{q}, \boldsymbol{k})$ given by Eq. (71), which enables us to predict three cases. Finally, we should mention that only in case (ii) the dynamical behavior in the experiments can be exactly described by the Brownian-dynamics simulations if time in experiments and that in simulations are scaled by $1/q^2 D_\alpha^S$ and $1/q^2 D_0$, respectively.

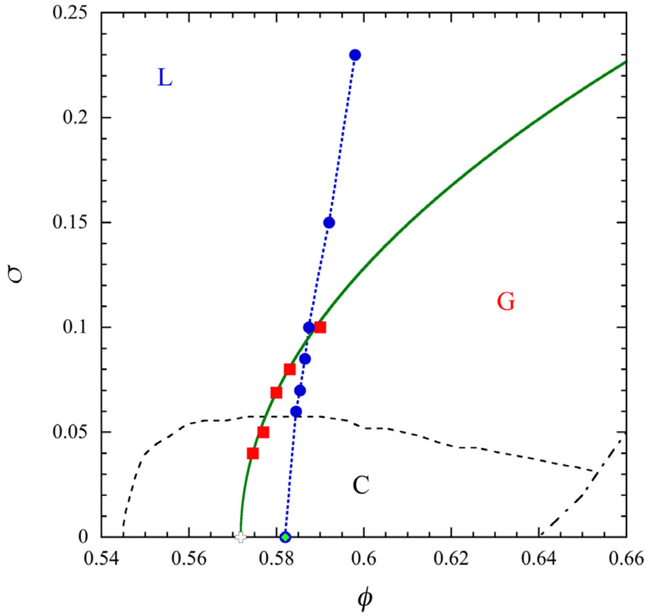

Fig. 2. (Color online) Phase diagram in volume fraction-polydispersity plane for polydisperse colloids. The symbols (□) indicate the critical points $\phi_c(\sigma)$ obtained from the experimental data for hard-sphere colloids, where the detailed values are listed in Table 1. The symbols (○) indicate the critical points $\phi_c^{(m)}(\sigma)$ obtained from the simulation results for hard spheres, (◊) the critical point $\phi_c^{(m)}(0)$ obtained by TMCT for PY model without the hydrodynamic interactions, and (+) the critical point $\phi_c(0)$ obtained by TMCT for PY model with the hydrodynamic interactions. The solid line indicates the hydrodynamic critical point $\phi_h(\sigma)$ given by Eq. (69), the dashed line the melting line obtained by the Monte Carlo simulation for hard spheres [60], the dot-dashed line the random close packing for hard spheres from Ref. [61], and the dotted lines among the critical points $\phi_c^{(m)}(\sigma)$ for a guide to eyes. L indicates a liquid state, C a crystal state, and G a glass state.

7. Summary

In this paper, we have derived the TMCT equation for the collective-intermediate scattering function $f(q, t)$ in colloidal suspensions by employing the same formulation as that used in molecular systems. Then, we have found the second-order differential equation for the cumulant function $K(q, t)$, where the nonlinear memory function contains the hydrodynamic correlation effect in addition to the mechanical correlation effect. Thus, we have explored how the long-range hydrodynamic interactions affect the critical volume fraction $\phi_c(\sigma)$ and predicted that there exist three cases for $\phi_c(\sigma)$, depending on the value of σ.

In order to check the existence of three cases, we have next investigated the critical volume fraction $\phi_c(\sigma)$ obtained from the four different experiments for suspensions of hard-sphere colloids for $0.04 \leq \sigma \leq 0.10$. Then, we have shown that all of them coincide with the hydrodynamic critical volume fraction $\phi_h(\sigma)$ within error, where three of them belong to cases (i) and one of them to (iii) (see Fig. 2). By using the hydrodynamic critical line given by Eq. (69) and the critical line of the simulations given by Eq. (76), we have also referred to a possibility of case (ii) where $\mathcal{F}_h(q) = 0$. In fact, as an intersection point of both lines, we have found $\sigma_0 \simeq 0.094866$ and $\phi_h(\sigma_0) = 0.58728$. Then, we have pointed out that if the Brownian-dynamics simulations and the experiments are done at $\sigma = \sigma_0$, both results are expected to coincide with each other since the hydrodynamic effects are canceled out. Thus, we emphasize that the long-range hydrodynamic interactions are indispensable to explain the experimental results for suspensions of polydisperse hard-sphere colloids. In order to confirm the theoretical prediction given by Eq. (75) from a unified point of view, however, one needs more experimental data for different values of σ. In fact, many data would be necessary to make an existence of three cases more clear because there exists at least 3% error on the observed values of ϕ [18].

Finally, we mention that the same formulation as that discussed in this paper is applicable to the systems with the non-direct interactions. However, it depends on the interactions whether the hydrodynamic interactions play an important role or not. For example, the Coulomb interactions between highly charged colloids are known to lead to the critical volume fraction ϕ_c much lower than ϕ_h [62,63]. In such systems, therefore, one can safely neglect the long-range hydrodynamic interactions even in a supercooled state since $\phi_c = \phi_c^{(m)} \ll \phi_h$. Otherwise, one needs to take into account the hydrodynamic effects seriously. This will be discussed elsewhere.

Appendix. Derivation of Eq. (8)

Starting from Eq. (4), one can then obtain

$$\frac{\partial}{\partial t}\Pi_{\boldsymbol{xp}}(t) = M(\boldsymbol{x},\boldsymbol{p})\Pi_{\boldsymbol{xp}}(t) + \Xi_{\boldsymbol{xp}}(t) \tag{A.1}$$

with the Fokker–Planck operator

$$\begin{aligned} M(\boldsymbol{x},\boldsymbol{p}) = &-\sum_{i=1}^{N}\left[\frac{\boldsymbol{p}_i}{m}\cdot\frac{\partial}{\partial \boldsymbol{x}_i} + \frac{\partial}{\partial \boldsymbol{p}_i}\cdot\sum_{j\neq i}^{N}\boldsymbol{F}_{ij}\right] \\ &+\sum_{i=1}^{N}\sum_{j=1}^{N}\frac{\partial}{\partial \boldsymbol{p}_i}\cdot\boldsymbol{\zeta}_{ij}\cdot\left[\frac{1}{m}\boldsymbol{p}_j + k_BT\frac{\partial}{\partial \boldsymbol{p}_j}\right], \end{aligned} \tag{A.2}$$

where the function $\Xi_{\boldsymbol{xp}}(t)$ denotes the additive type Gaussian, Markov noise and satisfies

$$\langle\Xi_{\boldsymbol{xp}}(t)\rangle = \langle\Xi_{\boldsymbol{xp}}(t)\Pi_{\boldsymbol{x'p'}}(0)\rangle = 0, \tag{A.3}$$

$$\langle\Xi_{\boldsymbol{xp}}(t)\Xi_{\boldsymbol{x'p'}}(0)\rangle = 2k_BT\delta(t)\sum_{i=1}^{N}\sum_{j=1}^{N}\frac{\partial}{\partial \boldsymbol{p}_i}\cdot\boldsymbol{\zeta}_{ij}\cdot\frac{\partial}{\partial \boldsymbol{p}'_j}\delta(\boldsymbol{x}-\boldsymbol{x}')\delta(\boldsymbol{p}-\boldsymbol{p}')p_e(\boldsymbol{x},\boldsymbol{p}). \tag{A.4}$$

Here $p_e(\boldsymbol{x},\boldsymbol{p})(=\langle\Pi_{\boldsymbol{xp}}(0)\rangle)$ denotes the equilibrium distribution function, which satisfies $M(\boldsymbol{x},\boldsymbol{p})p_e(\boldsymbol{x},\boldsymbol{p}) = 0$. The formal solution of Eq. (A.1) is given by

$$\Pi_{\boldsymbol{xp}}(t) = e^{tM}\Pi_{\boldsymbol{xp}}(0) + \int_0^t ds e^{(t-s)M}\Xi_{\boldsymbol{xp}}(s). \tag{A.5}$$

Then, one can write an arbitrary function $A_q(\boldsymbol{X}(t),\boldsymbol{P}(t))$ as

$$\begin{aligned} A_q(\boldsymbol{X}(t),\boldsymbol{P}(t)) &= \int d\boldsymbol{x}\int d\boldsymbol{p}A_q(\boldsymbol{x},\boldsymbol{p})\Pi_{\boldsymbol{xp}}(t) \\ &= \int d\boldsymbol{x}\int d\boldsymbol{p}[\Pi_{\boldsymbol{xp}}(0)e^{t\Lambda}A_q(\boldsymbol{x},\boldsymbol{p}) \\ &+ \int_0^t ds\Xi_{\boldsymbol{xp}}(t-s)e^{s\Lambda}A_q(\boldsymbol{x},\boldsymbol{p})], \end{aligned} \tag{A.6}$$

where Λ is the adjoint operator of the operator M given by

$$\Lambda(\boldsymbol{x},\boldsymbol{p})\delta(\boldsymbol{x}-\boldsymbol{x}')\delta(\boldsymbol{p}-\boldsymbol{p}') = M(\boldsymbol{x}',\boldsymbol{p}')\delta(\boldsymbol{x}-\boldsymbol{x}')\delta(\boldsymbol{p}-\boldsymbol{p}'). \tag{A.7}$$

Use of Eqs. (A.2) and (A.7) then leads to Eq. (9). Hence one can write the correlation function $\langle A_q(t)A_q(0)^*\rangle$ as

$$\langle A_q(\boldsymbol{X}(t),\boldsymbol{P}(t))A_q(\boldsymbol{X}(0),\boldsymbol{P}(0))^*\rangle = \langle A_q(\boldsymbol{x},\boldsymbol{p},t)A_q(\boldsymbol{x},\boldsymbol{p})^*\rangle_p, \tag{A.8}$$

where

$$A_q(\boldsymbol{x},\boldsymbol{p},t) = e^{t\Lambda}A_q(\boldsymbol{x},\boldsymbol{p}). \tag{A.9}$$

Here the brackets $\langle\cdots\rangle_p$ denote the average over the equilibrium distribution function $p_e(\boldsymbol{x},\boldsymbol{p})$. Since there is no difference between $\langle\cdots\rangle$ and $\langle\cdots\rangle_p$, therefore, in the following we just use the brackets $\langle\cdots\rangle$ instead of $\langle\cdots\rangle_p$ for simplicity. The variable $A_q(\boldsymbol{x},\boldsymbol{p},t)$ now obeys a new Eq. (8).

References

[1] P.N. Pusey, Light Scattering in Liquids and Macromolecular Solutions, Plenum Press, New York, 1980.
[2] P.N. Pusey, W. van Megen, Nature 320 (1986) 340.
[3] W. van Megen, S.M. Underwood, Phys. Rev. Lett. 70 (1993) 2766.
[4] W. van Megen, S.M. Underwood, Phys. Rev. Lett. 49 (1994) 4206.
[5] W. van Megen, Transp. Theory Stat. Phys. 24 (1995) 1017.
[6] S. Phan, W.B. Russel, Z. Cheng, J. Zhu, P.M. Chaikin, J.H. Dunsmuir, R.H. Ottewill, Phys. Rev. E 54 (1996) 6633.
[7] K.N. Pham, A.M. Puertas, J. Bergenholtz, S.U. Egelhaaf, A. Moussaïd, P.N. Pusey, A.B. Schofield, M.E. Cates, M. Fuchs, W.C.K. Poon, Science 296 (2002) 104.
[8] K.N. Pham, S.U. Egelhaaf, P.N. Pusey, W.C.K. Poon, Phys. Rev. E 69 (2004) 011503.
[9] A. Kasper, E. Bartsch, H. Sillescu, Langmuir 14 (1998) 5004.
[10] G. Brambilla, D. El Masri, M. Pierno, L. Berthier, L. Cipelletti, G. Petekidis, A.B. Schofield, Phys. Rev. Lett. 102 (2009) 085703.
[11] D. Heckendorf, K.J. Mutch, S.U. Egelhaaf, M. Laurati, Phys. Rev. Lett. 119 (2017) 048003.
[12] P.N. Pusey, in: J.P. Hansen, D. Levesque, J. Zinn-Justin (Eds.), Liquids, Freezing and Glass Transition, North-Holland, Amsterdam, 1991.

[13] J.C. Crocker, D.G. Grier, J. Colloid Interface Sci. 179 (1996) 298.
[14] W. van Megen, T.C. Mortensen, S.R. Williams, J. Müller, Phys. Rev. E 58 (1998) 6073.
[15] E.R. Weeks, J.C. Crocker, A.C. Levitt, A. Schofield, D.A. Weitz, Science 287 (2000) 627.
[16] S. Gupta, M. Camargo, J. Stellbrink, J. Allgaier, A. Radulescu, P. Lindner, E. Zaccarelli, C.N. Likos, D. Richter, Nanoscale 7 (2015) 13924.
[17] G.L. Hunter, E.R. Weeks, Rep. Progr. Phys. 75 (2012) 066501.
[18] W.C. Poon, E.R. Weeks, C.P. Royall, Soft Matter 8 (2012) 21.
[19] P. Mazur, Physica A 110 (1982) 128.
[20] M. Tokuyama, I. Oppenheim, Phys. Rev. E 50 (1994) R16.
[21] M. Tokuyama, I. Oppenheim, Physica A 216 (1995) 85.
[22] M. Medina-Noyola, Phys. Rev. Lett. 60 (1988) 2705.
[23] H. Löwen, Phys. Rep. 237 (1994) 249.
[24] R.A. Lionberger, W.B. Russel, J. Rheology 41 (1997) 399.
[25] G. Nägele, P. Baur, Europhys. Lett. 38 (1997) 557.
[26] M. Fuchs, W. Götze, M.R. Mayr, Phys. Rev. E 58 (1998) 3384.
[27] F. Sciortino, Nature Mater. 1 (2002) 145.
[28] I. Moriguchi, J. Chem. Phys. 106 (1997) 8624.
[29] M. Tokuyama, H. Yamazaki, Y. Terada, Phys. Rev. E 67 (2003) 062403.
[30] M. Tokuyama, H. Yamazaki, Y. Terada, Physica A 328 (2003) 367.
[31] M. Tokuyama, Y. Terada, J. Phys. Chem. B 109 (2005) 21357.
[32] M. Tokuyama, T. Narumi, E. Kohira, Physica A 385 (2007) 439.
[33] E. Zaccarelli, C. Valeriani, E. Sanz, W.C.K. Poon, M.E. Cates, P.N. Pusey, Phys. Rev. Lett. 103 (2009) 135704.
[34] L. Berthier, D. Coslovich, A. Ninarello, M. Ozawa, Phys. Rev. Lett. 116 (2016) 238002.
[35] B. Doliwa, A. Heuer, Phys. Rev. E 61 (2000) 6898.
[36] M. Hermes, M. Dijkstra, J. Phys.: Condens. Matter 22 (2010) 104114.
[37] M. Tokuyama, Phys. Rev. E 80 (2009) 031503.
[38] M. Rex, H. Löwen, Eur. Phys. J. E 28 (2009) 139.
[39] K.S. Schweizer, Curr. Opin. Colloid Interface Sci. 12 (2007) 297.
[40] E. Nazockdast, J.F. Morris, J. Fluid Mech. 713 (2012) 420.
[41] J. Mittal, G. Hummer, J. Chem. Phys. 137 (2012) 034110.
[42] B.D. Goddard, A. Nold, N. Savva, P. Yatsyshin, S. Kalliadasis, J. Phys.: Condens. Matter 25 (2013) 035101.
[43] R.N. Zia, J.W. Swan, Y. Su, J. Chem. Phys. 143 (2015) 224901.
[44] M. Tokuyama, Physica A 395 (2014) 31.
[45] M. Tokuyama, Physica A 430 (2015) 156.
[46] M. Tokuyama, Physica A 465 (2017) 229.
[47] M. Tokuyama, Physica A 484 (2017) 453.
[48] H. Mori, Progr. Theoret. Phys. 33 (1965) 423.
[49] M. Tokuyama, H. Mori, Progr. Theoret. Phys. 54 (1975) 918.
[50] M. Tokuyama, H. Mori, Progr. Theoret. Phys. 55 (1976) 411.
[51] R. Kubo, J. Phys. Soc. Japan 17 (1962) 1100.
[52] M. Tokuyama, I. Oppenheim, Physica A 94 (1978) 501.
[53] M. Tokuyama, Physica A 387 (2008) 4015.
[54] M. Tokuyama, Physica A 389 (2010) 951.
[55] U. Bengtzelius, W. Götze, A. Sjölander, J. Phys. C 17 (1984) 5915.
[56] W. Götze, R. Schilling, Phys. Rev. E 91 (2015) 042117.
[57] Y. Kimura, M. Tokuyama, Nuovo Cimento C 39 (2016) 300.
[58] T. Narumi, M. Tokuyama, Phys. Rev. E 95 (2017) 032601.
[59] J.K. Percus, G.J. Yevick, Phys. Rev. 110 (1958) 1.
[60] D.A. Kofke, P.G. Bolhuis, Phys. Rev. E 59 (1999) 618.
[61] W. Schaertl, H. Sillescu, J. Stat. Phys. 77 (1994) 1007.
[62] Ch. Beck, W. Härtl, R. Hempelmann, J. Chem. Phys. 111 (1999) 8209.
[63] M. Tokuyama, T. Furubayashi, J. Kawamura, Physica A 486 (2017) 681.